**Supporting TABLE 1. Sequences of shRNAs used.**

| Target | Sequences |
|---|---|
| **Human-sh*ABL1*-1** | CCGGGAGTTCTTGAAGCATTTCAAACTCGAGTTTGAAATGCTTCAAGAACTCTTTTTG |
| **Human-sh*ABL1*-2** | CCGGGCTTTGGGAAATTGCTACCTACTCGAGTAGGTAGCAATTTCCCAAAGCTTTTTG |
| **Human-sh*NOTCH1*** | CCGGCTTTGTTTCAGGTTCAGTATTCTCGAGAATACTGAACCTGAAACAAAGTTTTT |

**Supporting TABLE 2. Primary antibody information.**

| Antibody | Cat# | Company |
|---|---|---|
| ABL1 | 2862 | Cell Signaling |
| p-ABL1 (Tyr412) | 2865 | Cell Signaling |
| Phospho-AKT (Ser473) | 4060 | Cell signaling |
| AKT | 9272 | Cell Signaling |
| Phospho-ERK(Thr 202/Tyr 204) | 4370 | Cell Signaling |
| ERK | 4695 | Cell Signaling |
| NOTCH1 | 3608 | Cell Signaling |
| Phospho-c-Myc (Ser62) | 13748 | Cell Signaling |
| c-MYC | 5605 | Cell Signaling |
| CRKL | 3182 | Cell Signaling |
| p-CRKL (Tyr207) | 3181 | Cell Signaling |
| GAPDH | G8795 | Sigma |
| Ki67 | RM-9106-S0 | Fisher Scientific |
| NOTCH3 | 23426 | Abcam |
| AFP | A0008 | Dako |

**Supporting TABLE S3. Primer sequences used for RT-PCR.**

| Gene | Sequences |
|---|---|
| GAPDH-F | 5′-CTCTGGAAAGCTGTGGCGTGATG-3′ |
| GAPDH-R | 5′-ATGCCAGTGAGCTTCCCGTTCAG-3′ |
| NOTCH1-F | TGGACCAGATTGGGGAGTTC |
| NOTCH1-R | GCACACTCGTCTGTGTTGAC |
| NOTCH3-F | CGTGGCTTCTTTCTACTGTGC |
| NOTCH3-R | CGTTCACCGGATTTGTGTCAC |
| JAG1-F | GTCCATGCAGAACGTGAACG |

| | |
|---|---|
| JAG1-R | GCGGGACTGATACTCCTTGA |
| LFNG-F | GTCAGCGAGAACAAGGTGC |
| LFNG-R | GATCCGCTCAGCCGTATTCAT |
| DTX1-F | GACGGCCTACGATATGGACAT |
| DTX1-R | CCTAGCGATGAGAGGTCGAG |
| CCND1-F | GCTGCGAAGTGGAAACCATC |
| CCND1-R | CCTCCTTCTGCACACATTTGAA |
| Hes1-F | CCTGTCATCCCCGTCTACAC |
| Hes1-R | CACATGGAGTCCGCCGTAA |
| Hes2-F | CCAACTGCTCGAAGCTAGAGA |
| Hes2-R | AGCGCACGGTCATTTCCAG |
| NRARP-F | TCAACGTGAACTCGTTCGGG |
| NRARP-R | ACTTCGCCTTGGTGATGAGAT |
| NOTCH1 promoter-F | GAGCGCAGCGAAGGAACGA |
| NOTCH1 promoter-R | TCTCTTCCCCGGCTGGCT |



## Supporting Figure Legends

**Supporting Fig. S1**. **High expression of *ABL1* in human HCCs is positively correlated with poorer patient prognosis.**

Kaplan-Meier plot of overall survival of HCC patients stratified by *ABL1* mRNA expression level from TCGA database.

**Supporting Fig. S2**. **Deletion of *Abl1* in hepatocytes does not affect morphology, histology, proliferation, nor apoptosis in mouse liver.**
(**A**) Genotyping of Alb-Cre, Alb-Cre; *Abl1*$^{flox/+}$, and Alb-Cre; *Abl1*$^{flox/flox}$ mice. **(B)** Protein expression of ABL1 and GAPDH in whole liver tissues and isolated hepatocytes of Alb-Cre (Hep$^{WT}$) and Alb-Cre; *Abl1*$^{flox/flox}$ (Hep$^{Abl1-/-}$) mice was determined by Western blotting. **(C)** Photographs of livers from Hep$^{WT}$ and Hep$^{Abl1-/-}$ mice at 7 weeks of age. **(D)** Representative pictures of H&E-stained sections for (C). **(E)** Hepatic proliferation in the livers of 7 week-old Hep$^{WT}$ and Hep$^{Abl1-/-}$ mice was examined by immunohistochemistry for Ki67 protein expression. **(F)** Quantification of Ki67 staining (n=4). **(G)** Hepatic apoptosis in the livers of 7 week old Hep$^{WT}$ and Hep$^{Abl1-/-}$ mice was examined by TUNEL staining. **(H)** Quantification of TUNEL staining for (G) (n=4).

**Supporting Fig. S3**. ***ABL1* is not activated in DEN-induced HCC tumors.**
Expression of p-ABL1, ABL1, and GAPDH proteins in the livers of wild-type C57B6/J male mice 10 months after injection of DEN.

**Supporting Fig. S4**. **Comparable transfection efficiency of hydrodynamic injection in WT and *Abl1*-KO mouse liver.**
**(A)** GFP expression in the livers of 7 week-old Hep$^{WT}$ and Hep$^{Abl1-/-}$ mice (n=3/group) was examined by immunohistochemistry 7 days after injection of pT3-GFP. **(B)** Quantification of GFP staining (n=3/group).

**Supporting Fig. S5**. ***ABL1*** **is expressed in HCC cells.**
Relative *ABL1* mRNA levels in a number of HCC cell lines were examined by real-time PCR.

**Supporting Fig. S6**. **Knockout of *ABL1* decreases expression of NOTCH1 targets in MET/CAT-induced HCC tumors.**

**(A-C)** Relative *CyclinD1, Nrarp, and Hes1* mRNA levels in whole livers of $Hep^{WT}$ and $Hep^{Abl1-/-}$ mice treated with pT3-GFP or MET/CAT for 9 weeks was determined by real-time PCR.

**Supporting Fig. S7. miRNAs may not contribute to regulation of *NOTCH1* by ABL1.**
**(A)** Relative *miR-150-5p* mRNA levels in scrambled-RNA and *ABL1*-KD Huh7 cells. **(B)** Relative *miR-34a-5p* mRNA levels in scrambled-RNA and *ABL1*-KD Huh7 cells. **(C)** Relative *miR-146b-5p* mRNA levels in scrambled-RNA and *ABL1*-KD Huh7 cells. **(D)** Relative *miR-146b-5p* levels in Huh7 cells treated with miR146b-bp-mimic at different concentrations. **(E)** Relative *miR-146b-5p* levels in Huh7 cells treated with miR146b-bp inhibitors at different concentrations. **(F)** Expression of NOTCH1 and GAPDH proteins in Huh7 cells treated with control or *miR146b-5p-mimic* for 24h. **(G)** Expression of NOTCH1 and GAPDH proteins in scrambled-RNA and *ABL1*-KD Huh7 cells treated with control or *miR146b-5p* inhibitors for 24h.

**Supporting Fig. S8**. **Knockout of *ABL1* decreases expression of c-MYC in MET/CAT-induced HCC tumors.**
c-MYC expression in whole livers of $Hep^{WT}$ and $Hep^{Abl1-/-}$ mice treated with pT3-GFP or MET/CAT for 9 weeks was determined by Western blotting.

**Supporting Fig. S9**. **ABL1 interacts with c-MYC in HCC cells.**
The interaction of ABL1 and c-MYC was examined using proximity ligation assay (PLA) in Huh7 cells. PLA puncta per cell was quantified using Image J.

**Supporting Fig. S10. Neither knockdown nor overexpression of *NOTCH1* affects expression of c-MYC protein in HCC cells.**
Expression of c-MYC, NOTCH1 and GAPDH proteins in Huh7 cells infected with scrambled-shRNA, NOTCH1-shRNA, EF.CMV.GFP (control) or EF.hICN1.CMV.GFP (NOTCH1-OE).

**Supportng Fig. S11. c-MYC directly binds to the promoter of *NOTCH1* in human HCC cells.**
**(A)** Putative transcription factor binding sites human *NOTCH1* promoter were analyzed by TFsearch software. **(B)** ChIP-PCR analysis reveals the binding of c-MYC to the *NOTCH1* promoter in Huh7 cells. **(C)** ChIP-qPCR analysis reveals the binding of c-MYC to the *NOTCH1* promoter in Huh7 cells.

**Supporting Fig. S12. *c-MYC* mRNA level has no correlation with *ABL1* or *NOTCH1* mRNA levels in TCGA HCC samples.**
**(A)** Correlation of *c-MYC* and *ABL1* mRNA in HCC samples from the TCGA database was analyzed. **(B)** Correlation of *c-MYC* and *NOTCH1* mRNAs in HCC samples from the TCGA database was analyzed.

**Supporting Fig. S13. ABL inhibitors inhibit HCC cell growth.**
**(A)** Expression of p-CRKL (a direct target of ABL1), CRKL and GAPDH proteins in Hep3B and Huh7 cells treated with vehicle or 3μM nilotinib for 4h or 24h. **(B)** Expression of p-CRKL, CRKL, and GAPDH proteins in Huh7 cells treated with vehicle or 20μM GNF5 for 4h or 24h. **(C)**

Quantification of cell proliferation of Hep3B and Huh7 cells treated with vehicle or GNF-5 at different time points after treatment.

**Supporting Fig. S14. Nilotinib treatment decreases HCC cell growth.** **(A)** $IC_{50}$ for nilotinib in 8 HCC cell lines was calculated for cell growth experiment described in Figure 7A using non-linear regression. **(B)** Expression of ABL1, c-MYC, NOTCH1 and GAPDH proteins in 8 HCC cells. **(C)** Correlation between c-MYC (left) and NOTCH1 (right) protein expression and ABL1 protein expression in 8 HCC cell lines. **(D)** Correlation between NOTCH1 protein expression and ABL1 protein expression in HCC cells with or without p53 mutations.

**Supporting Fig. S15. Nilotinib treatment decreases HCC cell proliferation in a xenograft model.**
**(A)** Ki67 staining of tumors from Huh7 cells treated with vehicle or nilotinib was examined by IHC. **(B)** Quantification of Ki67 staining (n=3/group). **(C)** TUNEL staining of Huh7 xenograft tumors treated with vehicle or nilotinib was examined by IHC. **(D)** Quantification of TUNEL staining (n=3/group).

**Supporting Fig. S16. Nilotinib treatment decreases HCC cell proliferation in the MET/CAT model.**
**(A)** Diagram of the experimental protocol. **(B)** Ki67 and AFP staining of tumors induced by MET/CAT treated with vehicle or nilotinib was examined by IHC.

**Supporting Fig. S17. Sorafenib is not effective in suppressing tumor growth in the MET/CAT-induced HCC model.**
**(A)** Diagram of the experimental protocol. **(B)** Gross images of tumors from vehicle- (left) and sorafenib-treated animals (right) are shown. **(C)** Body weight ratios of mice after/before sorafenib treatment (n=6/group). **(D)** Kaplan-Meyer survival graph for mice treated with vehicle or sorafenib (n=6/group).

**Supporting Fig. S18. *ABL1* expression is correlated with expression of c-MET-activated genes.**
Correlation between *ABL1* mRNA expression and the expression of genes (*FGD6, ITGB1, ITGAV, NCK2, ANXA5, and KPNB1*) from "the c-MET activation gene set" in human HCCs from the TCGA database.

**Supporting Fig. S19. Neither knockdown nor overexpression of *NOTCH1* affects phosphorylation of AKT or ERK in HCC cells.**
Expression of p-AKT, AKT, p-ERK, ERK, ABL1, p-CRKL, and GAPDH proteins in Huh7 cells infected with scrambled-RNA or *ABL1*-KD Huh7 cells.

**Supporting Fig. S20. *ABL1* knockdown downregulates a number of signaling pathways.**
GSEA reveals down-regulation of several gene sets, including hypoxia, the p53 pathway, estrogen response, glycolysis, androgen response, and spermatogenesis by knockdown of *ABL1* in Huh7 cells.

## Supporting Experimental Procedures

### Cells and reagents

Huh7, Hep3B, PLC/PRF/5, Skep-1, and 293T cells were cultured in Dulbecco's modified Eagle's medium (DMEM, high glucose, Thermo Scientific, Waltham, MA), supplemented with 10% fetal bovine serum (FBS, Tissue Culture Biologicals), penicillin, and streptomycin (Sigma-Aldrich, St. Louis, MO) in a humidified atmosphere of 5% $CO_2$ at 37°C. SNU387, SNU423, SNU449 and SNU475 were cultured in RPMI 1640 medium supplemented with 10% fetal bovine serum (Tissue Culture Biologicals), 1x penicillin/streptomycin (Sigma-Aldrich, St. Louis, MO) at 37°C and 5% CO2.

### TCGA data analysis

The data for all boxplots and correlation plots were retrieved from the UCSC Xena platform (https://xenabrowser.net/), specifically from the TCGA Liver Cancer (LIHC) study. For the first variable, the data type selected was "Genomic" and the Assay Type selected was "Gene Expression". For the second variable, the data type selected was "Phenotypic". To create the boxplots in R 3.6.0, gene expression values were first separated into the categories Normal Tissue, consisting of Solid Tissue Normal samples, and Tumor Tissue, consisting of Primary Tumor and Recurrent Tumor samples. These sorted data were then plotted using the function boxplot. *p*-values were generated using Welch's *t*-test on two-sample, unpaired data. Normality required for all *t*-tests was assumed by central limit theorem and visual inspection of boxplots. The correlation plots were created using GraphPad Prism 8.0.1. The Pearson's coefficient of correlation, *R*, and its respective *p*-value (two-tailed) were also calculated by GraphPad Prism 8.0.1.

The data for Kaplan-Meier plots was retrieved from the Pathology Atlas section of the Human Protein Atlas (https://www.proteinatlas.org/humanproteome/pathology). Liver cancer TCGA RNA Sample, Description, and FPKM data were used for each individual gene. To create the Kaplan-Meier plots, Python 3.0 was used to modify the original data from the Pathology Atlas. Specifically, censored data were generated by dividing patients into two groups, in which the censored group consisted of patients who had not died by the end of the study time. Patient data were also separated into two different groups based on the expression level indicated by FKPM values, for which the dividing threshold was provided by the Pathology Atlas. Binary censored data, binary expression group data, and survival times were imported into R 3.6.0, where Kaplan-Meier plots were created using the survival, survminer, dplyr packages and the Surv, survfit, and ggsurvplot functions. *p*-values were generated by including the command "pval = TRUE" in the ggsurvplot function from the survminer library. Based on the FPKM value of each gene, patients were classified into two groups and association between prognosis (survival) and gene expression (FPKM) was examined. The best expression cut-off refers the FPKM value that yields maximal difference with regard to survival between the two groups at the lowest log-rank P-value. Best expression cut-off was selected based on survival analysis. If FPKM values were greater or equal to the best expression cut off value, they were defined as

high. If they were lower than this they were defined as low. We also used the median (50%) group cutoff method and found similar results.

### MET/CAT-induced HCC Model

For the MET/CAT-driven HCC model, 50µg of total plasmids, encoding the Sleeping Beauty transposase (HSB2) and transposons with GFP (pT3-GFP) or MET gene and catenin beta 1 gene with the N terminal truncation (referred to here as MET/CAT) (22.5µg pT3-EF1a-MET, 22.5µg pT3-EF1a-ΔN90-β-Catenin, and 5µg HSB2) were injected hydrodynamically into age- and gender-matched mice as described previously[1, 2]. All mice were maintained on the standard diet until being euthanized.

## Proximity Ligation Assay

Proximity ligation assay (PLA) was performed using the Duolink® In Situ Red Starter Kit Mouse/Rabbit (Millipore Sigma) according to the manufacturer's instructions. In brief, cells were seeded onto an 8 well-Nunc™ Lab-Tek™ II CC2™ Chamber Slide System (Thermo Fisher) at $17.5x10^3$/well overnight, then fixed with 4% paraformaldehyde for 30 min. at room temperature and washed in PBS, followed by permeabilization with 0.1% Triton X-100 for 10 min. After washing with Wash Buffer A (Millipore Sigma) followed by blocking with Duolink Blocking Buffer (Millipore Sigma) for 30 min. at room temperature, cells were incubated with primary antibodies (ABL1, # 2862, 1:100, Cell Signaling and c-MYC, #5605, 1:100, Cell Signaling) overnight at 4°C. The following day, cells were washed repeatedly in Wash Buffer A, followed by incubation with appropriate Duolink secondary antibodies (Millipore Sigma) for 1 hour at 37°C. According to the manufacturer's protocol. After washing with Wash Buffer A at room temperature, ligation and amplification steps of the PLA were performed according to the manufacturer's protocol. After final washes with Wash Buffer B at room temperature, slides were mounted with Corning® 24x50 mm Rectangular #1 Cover Glass (Corning) using Duolink® In Situ Mounting Medium with DAPI (Millipore Sigma).



1. Patil MA, Lee SA, Macias E, et al. Role of cyclin D1 as a mediator of c-Met- and beta-catenin-induced hepatocarcinogenesis. Cancer Res 2009;69:253-61.

2. Shang N, Arteaga M, Zaidi A, et al. FAK is required for c-Met/beta-catenin-driven hepatocarcinogenesis. Hepatology 2015;61:214-26.

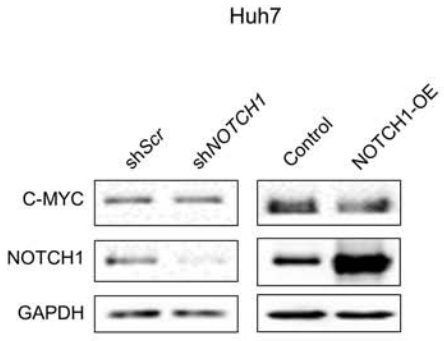
Huh7
shScr
shNOTCH1
Control
NOTCH1-OE
C-MYC
NOTCH1
GAPDH

A

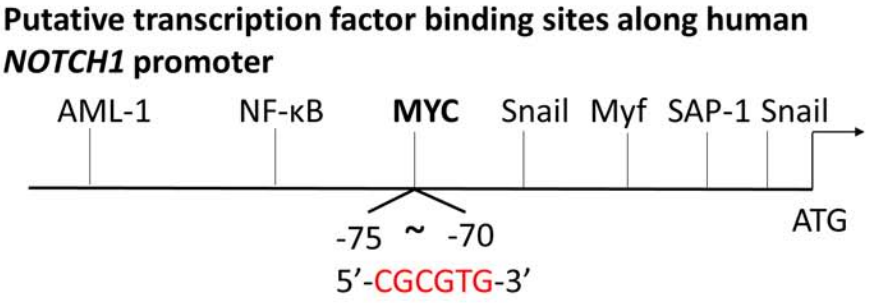
Putative transcription factor binding sites along human
NOTCH1 promoter
AML-1
NF-κB
MYC
Snail
Myf
SAP-1
Snail
ATG
-75 ~ -70
5'-CGCGTG-3'

B

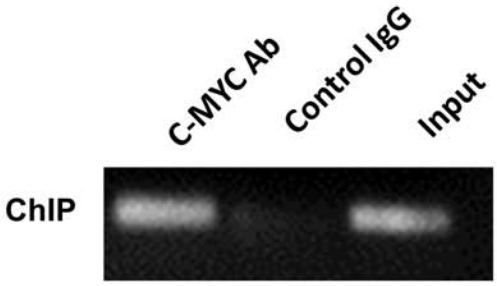
C-MYC Ab
Control IgG
Input
ChIP

C

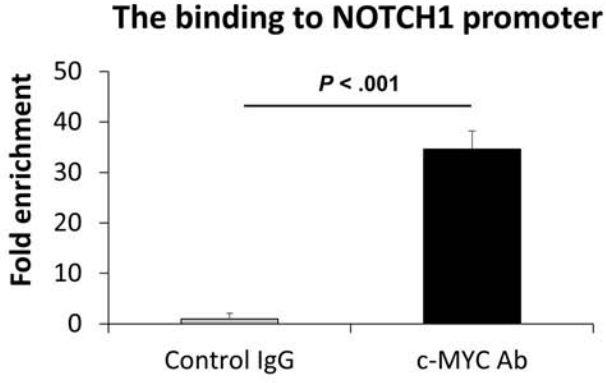
The binding to NOTCH1 promoter
P < .001
Fold enrichment
50
40
30
20
10
0
Control IgG
c-MYC Ab

A

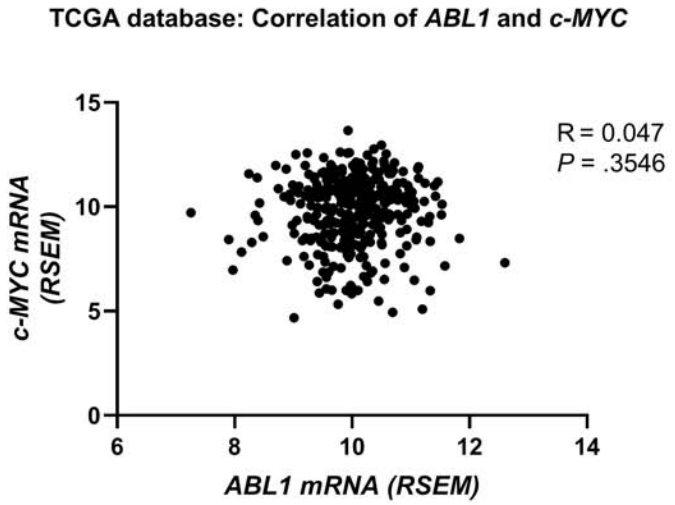
TCGA database: Correlation of ABL1 and c-MYC
R = 0.047
P = .3546
c-MYC mRNA (RSEM)
ABL1 mRNA (RSEM)
0
5
10
15
6
8
10
12
14

B

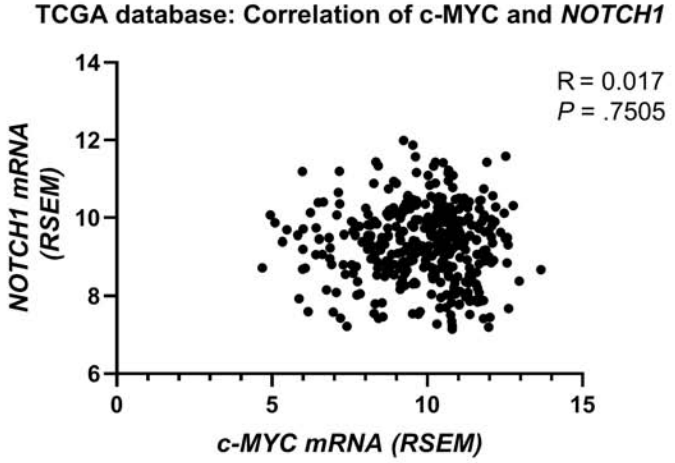
TCGA database: Correlation of c-MYC and NOTCH1
R = 0.017
P = .7505
NOTCH1 mRNA (RSEM)
c-MYC mRNA (RSEM)
6
8
10
12
14
0
5
10
15

A

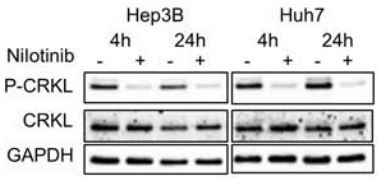
Hep3B
Huh7
4h
24h
4h
24h
Nilotinib
- + - + - + - +
P-CRKL
CRKL
GAPDH

B

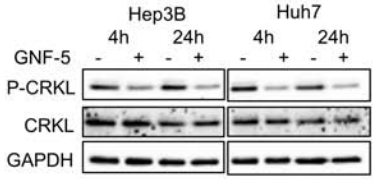
Hep3B
Huh7
4h
24h
4h
24h
GNF-5
- + - + - + - +
P-CRKL
CRKL
GAPDH

C

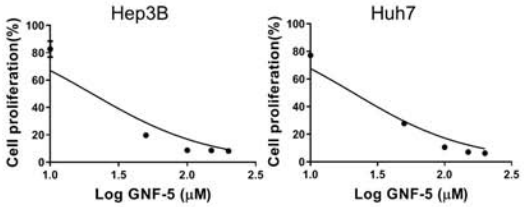
Hep3B
Huh7
Cell proliferation(%)
100
80
60
40
20
0
1.0
1.5
2.0
2.5
Log GNF-5 (μM)

A **IC50 for Nilotinib**

| Cell lines | Hep3B | SK-Hep1 | Huh7 | SNU-423 | SNU-449 | SNU-475 | PLC/PRF/5 | SNU-387 |
|---|---|---|---|---|---|---|---|---|
| IC50 (μM) | 5.02 | 6.15 | 5.88 | 11.03 | 11.69 | 6.93 | 11.2 | 10.2 |

B

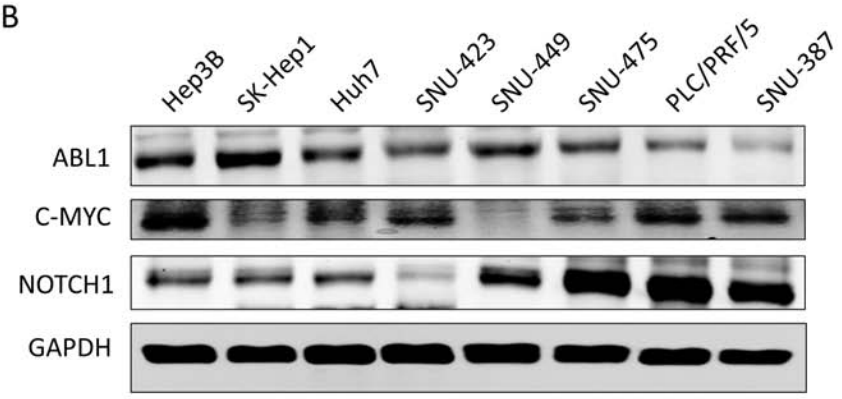


C

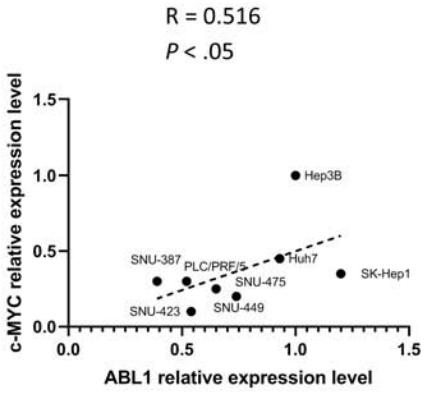


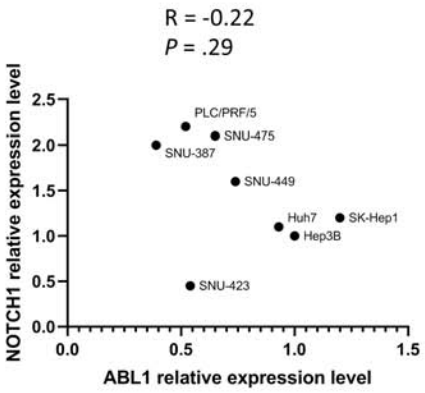


D

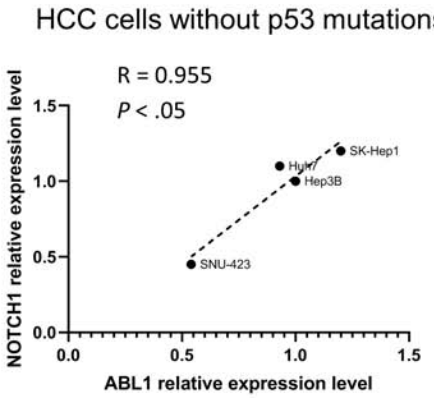


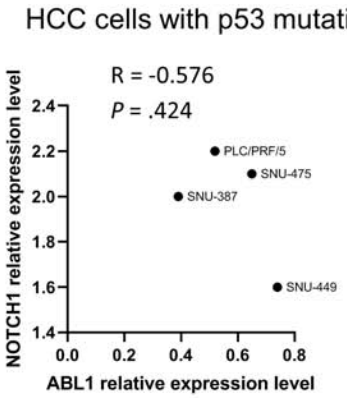

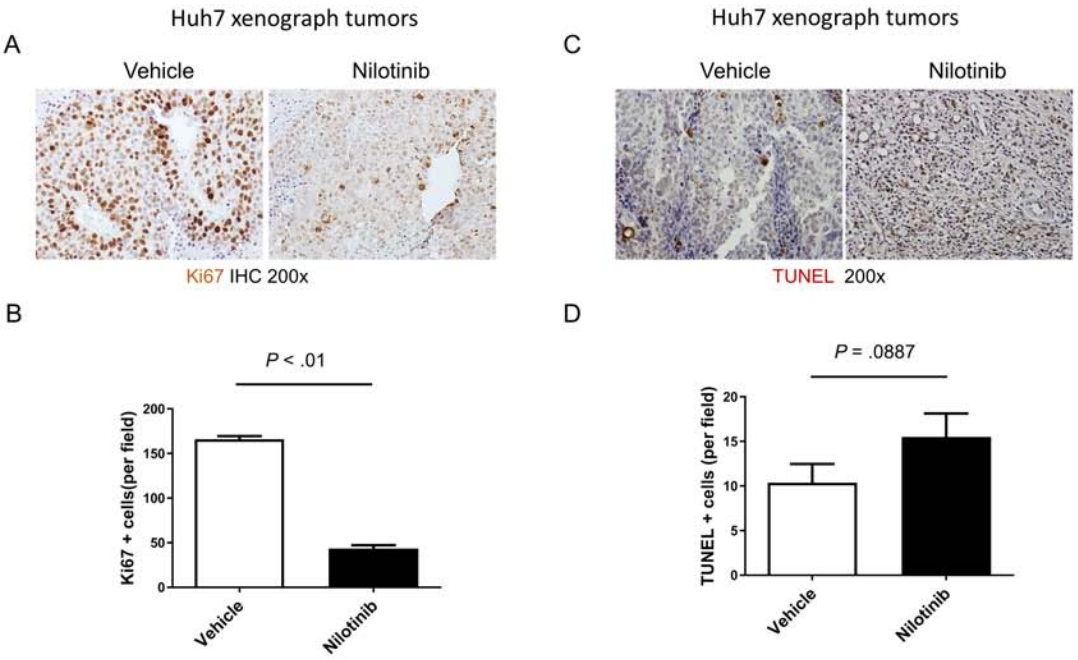
A
Huh7 xenograph tumors
Vehicle
Nilotinib
Ki67 IHC 200x
B
P < .01
Ki67 + cells(per field)
200
150
100
50
0
Vehicle
Nilotinib
C
Huh7 xenograph tumors
Vehicle
Nilotinib
TUNEL 200x
D
P = .0887
TUNEL + cells (per field)
20
15
10
5
0
Vehicle
Nilotinib

A

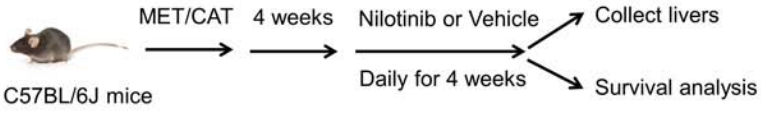
MET/CAT
4 weeks
Nilotinib or Vehicle
Collect livers
Daily for 4 weeks
Survival analysis
C57BL/6J mice

B

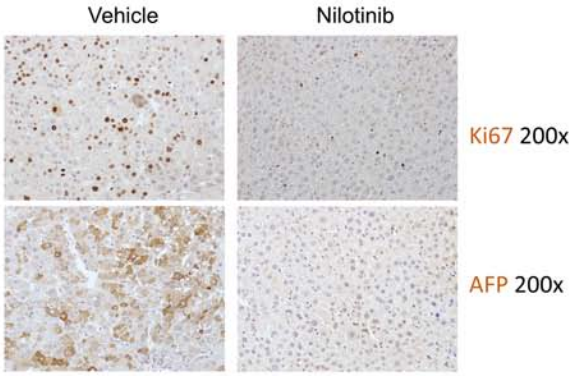
Vehicle
Nilotinib
Ki67 200x
AFP 200x
MET/CAT 8 weeks

A

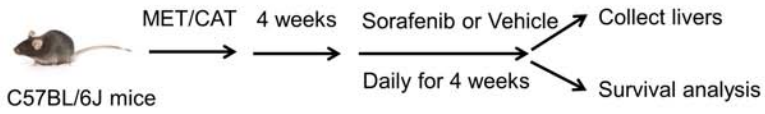
MET/CAT
4 weeks
Sorafenib or Vehicle
Collect livers
Daily for 4 weeks
Survival analysis
C57BL/6J mice

B


Vehicle
Sorafenib

C

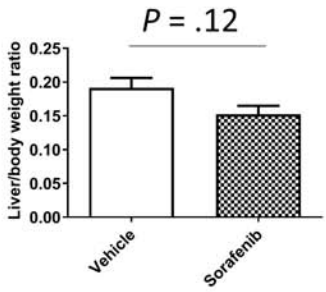
P = .12
Liver/body weight ratio
0.25
0.20
0.15
0.10
0.05
0.00
Vehicle
Sorafenib

D

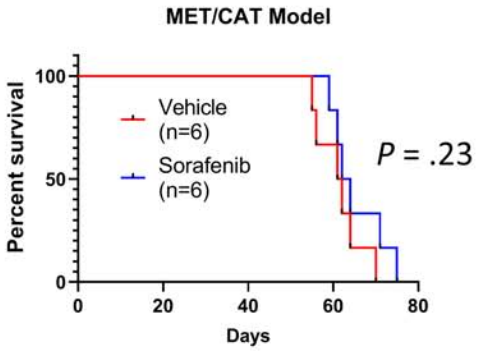
MET/CAT Model
Percent survival
100
50
0
Vehicle
(n=6)
Sorafenib
(n=6)
P = .23
0
20
40
60
80
Days

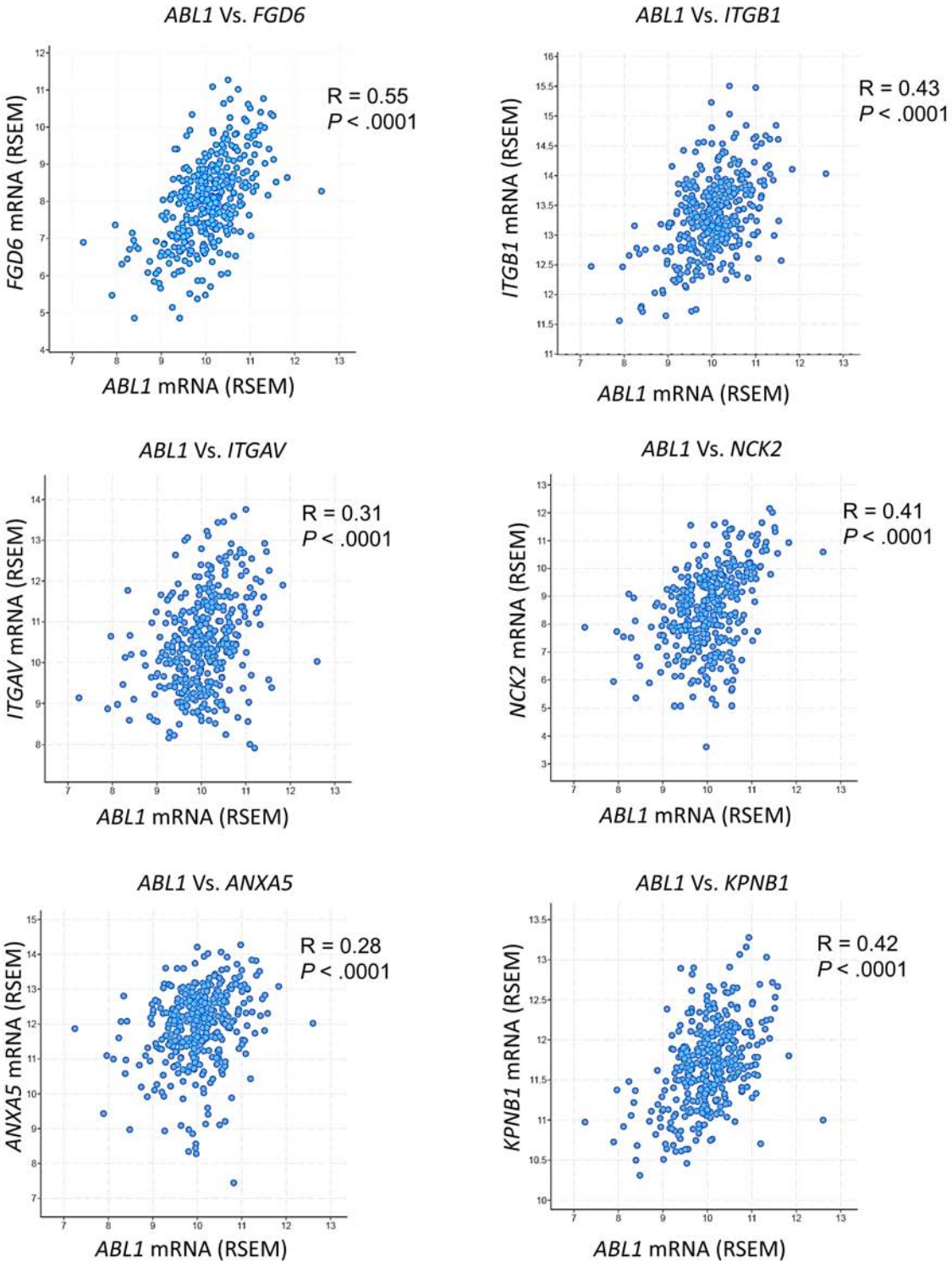
ABL1 Vs. FGD6
R = 0.55
P < .0001
FGD6 mRNA (RSEM)
ABL1 mRNA (RSEM)
ABL1 Vs. ITGB1
R = 0.43
P < .0001
ITGB1 mRNA (RSEM)
ABL1 mRNA (RSEM)
ABL1 Vs. ITGAV
R = 0.31
P < .0001
ITGAV mRNA (RSEM)
ABL1 mRNA (RSEM)
ABL1 Vs. NCK2
R = 0.41
P < .0001
NCK2 mRNA (RSEM)
ABL1 mRNA (RSEM)
ABL1 Vs. ANXA5
R = 0.28
P < .0001
ANXA5 mRNA (RSEM)
ABL1 mRNA (RSEM)
ABL1 Vs. KPNB1
R = 0.42
P < .0001
KPNB1 mRNA (RSEM)
ABL1 mRNA (RSEM)

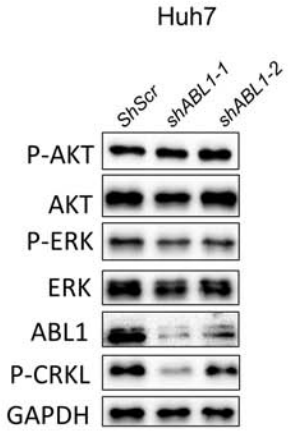
Huh7
ShScr
shABL1-1
shABL1-2
P-AKT
AKT
P-ERK
ERK
ABL1
P-CRKL
GAPDH

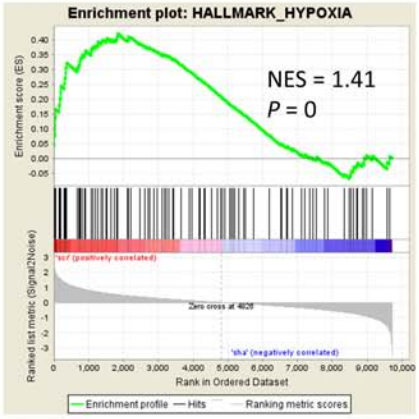
Enrichment plot: HALLMARK_HYPOXIA
NES = 1.41
P = 0
Enrichment score (ES)
Ranked list metric (Signal2Noise)
'scr' (positively correlated)
Zero cross at 4626
'sha' (negatively correlated)
Rank in Ordered Dataset
Enrichment profile
Hits
Ranking metric scores

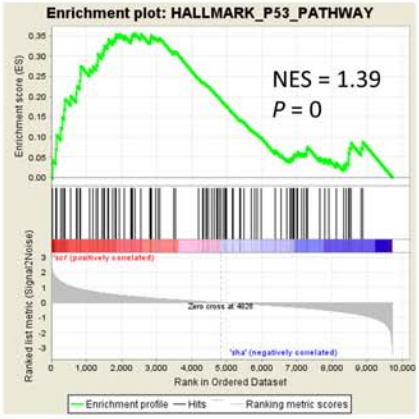
Enrichment plot: HALLMARK_P53_PATHWAY
NES = 1.39
P = 0
Enrichment score (ES)
Ranked list metric (Signal2Noise)
'scr' (positively correlated)
Zero cross at 4626
'sha' (negatively correlated)
Rank in Ordered Dataset
Enrichment profile
Hits
Ranking metric scores

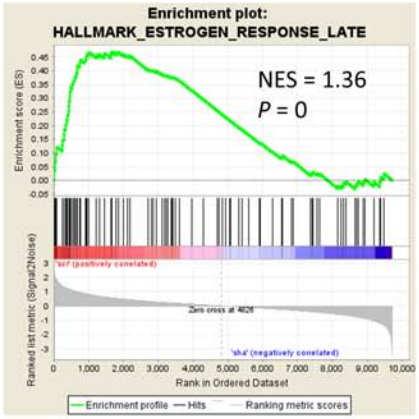
Enrichment plot:
HALLMARK_ESTROGEN_RESPONSE_LATE
NES = 1.36
P = 0
Enrichment score (ES)
Ranked list metric (Signal2Noise)
'scr' (positively correlated)
Zero cross at 4626
'sha' (negatively correlated)
Rank in Ordered Dataset
Enrichment profile
Hits
Ranking metric scores

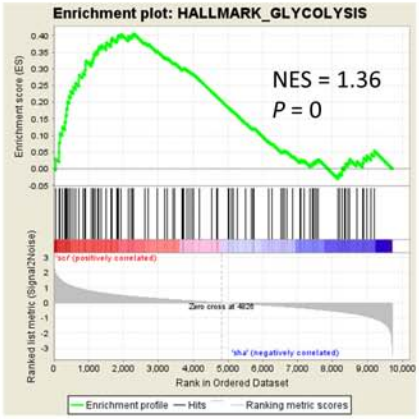
Enrichment plot: HALLMARK_GLYCOLYSIS
NES = 1.36
P = 0
Enrichment score (ES)
Ranked list metric (Signal2Noise)
'scr' (positively correlated)
Zero cross at 4626
'sha' (negatively correlated)
Rank in Ordered Dataset
Enrichment profile
Hits
Ranking metric scores

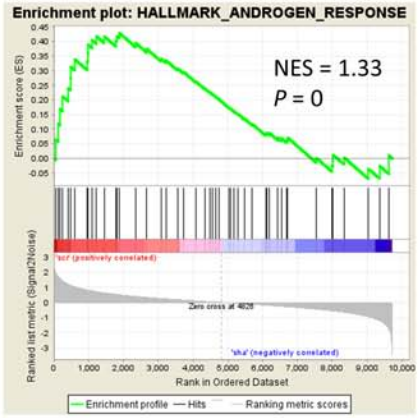
Enrichment plot: HALLMARK_ANDROGEN_RESPONSE
NES = 1.33
P = 0
Enrichment score (ES)
Ranked list metric (Signal2Noise)
'scr' (positively correlated)
Zero cross at 4626
'sha' (negatively correlated)
Rank in Ordered Dataset
Enrichment profile
Hits
Ranking metric scores

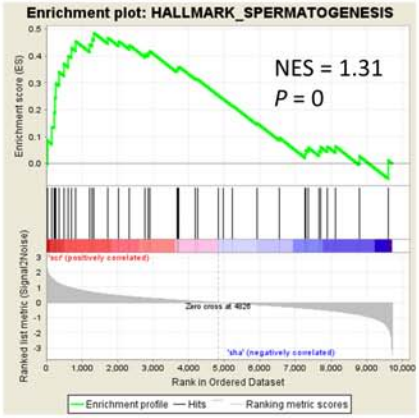
Enrichment plot: HALLMARK_SPERMATOGENESIS
NES = 1.31
P = 0
Enrichment score (ES)
Ranked list metric (Signal2Noise)
'scr' (positively correlated)
Zero cross at 4626
'sha' (negatively correlated)
Rank in Ordered Dataset
Enrichment profile
Hits
Ranking metric scores

A

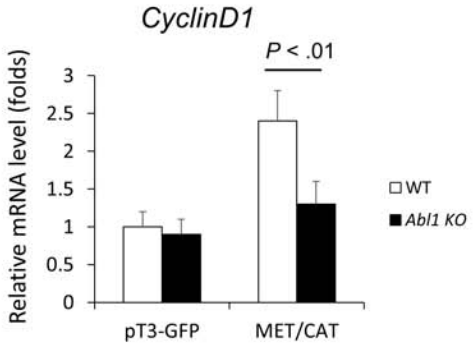
CyclinD1
P < .01
Relative mRNA level (folds)
3
2.5
2
1.5
1
0.5
0
pT3-GFP
MET/CAT
WT
Abl1 KO

B

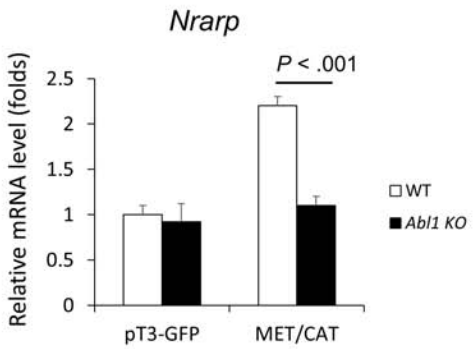
Nrarp
P < .001
Relative mRNA level (folds)
2.5
2
1.5
1
0.5
0
pT3-GFP
MET/CAT
WT
Abl1 KO

C

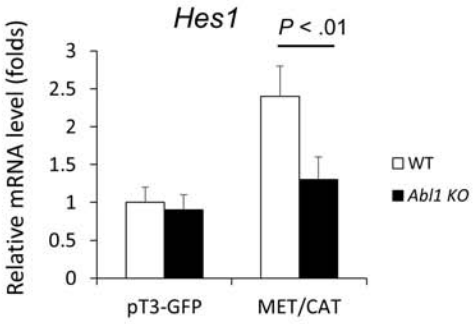
Hes1
P < .01
Relative mRNA level (folds)
3
2.5
2
1.5
1
0.5
0
pT3-GFP
MET/CAT
WT
Abl1 KO

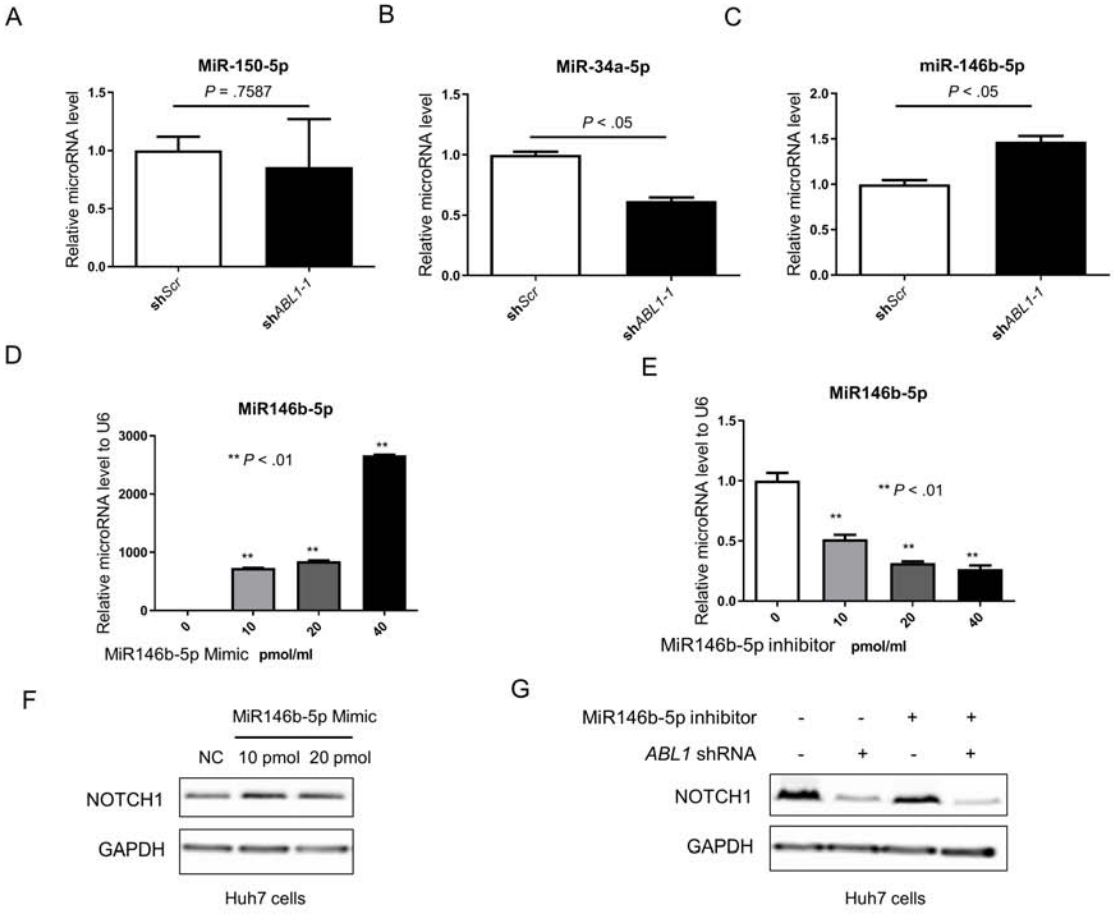
A
MiR-150-5p
P = .7587
Relative microRNA level
shScr
shABL1-1
B
MiR-34a-5p
P < .05
C
miR-146b-5p
P < .05
D
MiR146b-5p
** P < .01
Relative microRNA level to U6
MiR146b-5p Mimic pmol/ml
E
MiR146b-5p
** P < .01
MiR146b-5p inhibitor pmol/ml
F
MiR146b-5p Mimic
NC 10 pmol 20 pmol
NOTCH1
GAPDH
Huh7 cells
G
MiR146b-5p inhibitor
ABL1 shRNA
NOTCH1
GAPDH
Huh7 cells

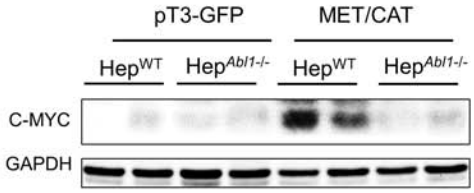
pT3-GFP
MET/CAT
Hep^WT
Hep^Abl1-/-
Hep^WT
Hep^Abl1-/-
C-MYC
GAPDH

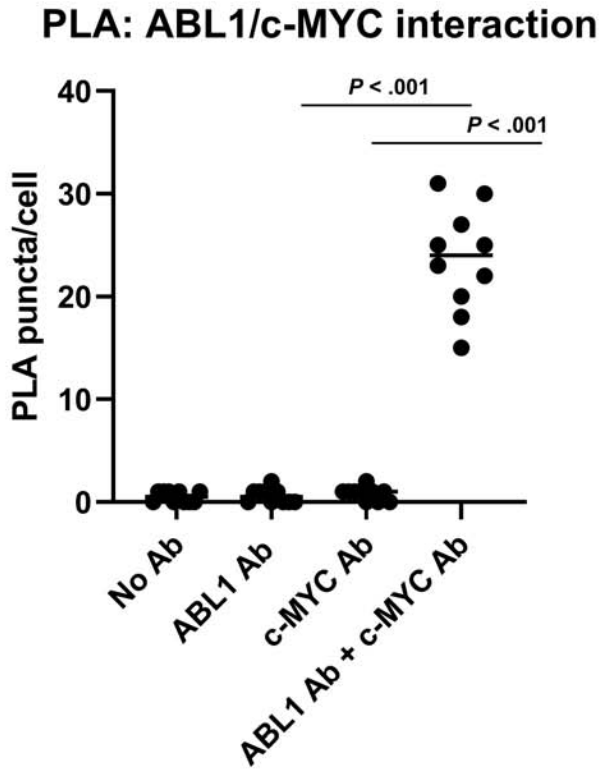
PLA: ABL1/c-MYC interaction
P < .001
P < .001
PLA puncta/cell
40
30
20
10
0
No Ab
ABL1 Ab
c-MYC Ab
ABL1 Ab + c-MYC Ab

**What you need to know:**

BACKGROUND AND CONTEXT: The oncogene ABL1 might be involved in the pathogenesis of hepatocellular carcinoma (HCC).

NEW FINDINGS: HCC samples have increased levels of ABL1 compared with non-tumor liver tissues, and loss or inhibition of ABL1 reduces proliferation of HCC cells and slows growth of tumors in mice.

LIMITATIONS: This study was performed using human tissue samples, cell lines, and mice. Further studies in humans are needed.

IMPACT: Inhibitors of ABL1 might be developed for treatment of HCC

**Lay Summary**: We identified a protein that is upregulated in human HCC samples. When we deleted or inhibited this protein in mice, liver tumors grew more slowly and the mice had longer survival times.